

# Microstructure and Mechanical Properties of As-extruded and Heat-treated Mg-6Zn-1Mn-2Sn-0.5Ca

Chen Xia<sup>1,2</sup>, Zhang Dingfei<sup>1,2</sup>, Feng Jingkai<sup>1,2</sup>, Zhao Yang<sup>1,2</sup>, Jiang Bin<sup>1,2</sup>,  
Pan Fusheng<sup>2,3</sup>

<sup>1</sup> College of Materials Science and Engineering, Chongqing University, Chongqing 400044, China; <sup>2</sup> National Engineering Research Center for Magnesium Alloys, Chongqing University, Chongqing 400044, China; <sup>3</sup> Chongqing Academy of Science and Technology, Chongqing 401123, China

**Abstract:** The microstructures and mechanical properties of as-extruded and peak-aged Mg-6Zn-1Mn-2Sn-0.5Ca (ZMT612-0.5Ca) alloy were studied by optical microscopy (OM), X-ray diffractometer (XRD), scanning electron microscopy (SEM), transmission electron microscopy (TEM), hardness tests and uniaxial tensile tests. The results show that the as-cast alloy consists of  $\alpha$ -Mg, Mn, Mg<sub>7</sub>Zn<sub>3</sub>, Ca<sub>2</sub>Mg<sub>6</sub>Zn<sub>3</sub> and CaMgSn phases. The as-extruded ZMT612-0.5Ca alloy presents a totally recrystallized microstructure. The average grain size of extruded alloy is  $\sim 2.8 \mu\text{m}$ . After heat treatment, the strength increases obviously, and the yield strength and ultimate tensile strength of as-extruded alloy are increased to 320 and 390 MPa, respectively. Strength enhancement is attributed to the grain boundary strengthening, solid solution strengthening and precipitation strengthening.

**Key words:** Mg-Zn-Mn-Sn-Ca; extrusion; peak-aged; microstructure; mechanical properties

Magnesium (Mg) alloys have a good application prospects in auto-mobile, aircraft, aerospace, and 3C industries due to their low density ( $\sim 1/4$  of steel and  $\sim 3/5$  of aluminum), high specific strength, high specific stiffness and good damping ability. However, the applications of Mg alloys are still restricted for their poor strength and ductility compared with aluminum (Al) alloys and steels<sup>[1-3]</sup>. As we all know, adding rare earth (RE) elements is considered to be an effective approach to improve strength of Mg alloys. Some commercially used RE in Mg alloys include gadolinium (Gd), cerium (Ce) and yttrium (Y), etc<sup>[4-6]</sup>. For example, Mg-2.5Zn-6.8Y with 600 MPa strength has been reported in Akihisa's research<sup>[7]</sup>. However, adding a lot of RE elements causes the increase of cost and density of the alloys, which is unacceptable in commercial applications. Hence, the development of new magnesium alloys based on partial or complete substitution of RE by other elements is extremely necessary.

Mg-Zn-Sn alloys are typically age-hardenable wrought Mg alloys, which have great potential to improve the strength by various heat treatments and alloying<sup>[8]</sup>. It has been reported that the hardness of Mg-2.2Sn-0.5Zn alloy increases significantly after aging treatment<sup>[9]</sup>. In our previous study, the effects of Sn on Mg-6Zn-1Mn(ZM61) alloy have been researched and Mg-6Zn-1Mn-4Sn alloy is found to own the best mechanical properties in Mg-6Zn-1Mn- $x$ Sn ( $x=1, 2, 4, 6, 8, 10$ )<sup>[10]</sup> due to the second phase Mg<sub>2</sub>Sn which has high hardness, high melting point, and good thermal stability. However, the effect of coarse and sparsely distributed Mg<sub>2</sub>Sn to the strength is restricted and Sn element is not cheap, so low Sn content alloys with high strength are expected. Besides, Ca element, with a high growth restriction factor (GRF), is believed to be a very attractive and cheap element to refine grain size<sup>[11]</sup>. Chang et al<sup>[12]</sup> suggested that Ca refines the micro-sized and nano-sized Mg<sub>2</sub>Sn when it is added into Mg-5Sn-3Zn alloy.

Received date: September 20, 2019

Foundation item: National Key Research and Development Program of China (2016YFB0301101); National Natural Science Foundation of China (51571040, U1764253, 51531002)

Corresponding author: Zhang Dingfei, Ph. D., Professor, College of Materials Science and Engineering, Chongqing University, Chongqing 400044, P. R. China, Tel: 0086-23-65112491, E-mail: zhangdingfei@cqu.edu.cn

Copyright © 2020, Northwest Institute for Nonferrous Metal Research. Published by Science Press. All rights reserved.

Zhang<sup>[13]</sup> also found that Mg-6Sn alloys are refined by the addition of Zn and Ca elements. Pan<sup>[14]</sup> developed TX22 which is low-alloyed and rare-earth-free magnesium alloys with ultra-high strength. The Ca addition promotes accumulation of the pyramidal dislocations, and the solute Ca segregation and nano-precipitates can block the motion of low angle grain boundaries (LAGBs). Ca and Sn are readily to form CaMgSn with high melting point in Mg alloys, and the influence of this phase on aging response of Mg-Sn-Zn-Ca alloy has been reported by Wahid et al<sup>[15]</sup>; they found that the CaMgSn can act as a nucleation site for Mg<sub>2</sub>Sn and MgZn phases during the aging process due to its high energy interface with the Mg matrix. So it is interest to develop Mg-Zn-Sn-Ca alloys based on ZM61 alloy. However, to the author's knowledge, few detailed research has been conducted on the microstructures and mechanical properties of ZM61-Sn-Ca. Therefore, we developed a new high strength Mg-6Zn-1Mn-2Sn-0.5Ca.

In this work, the microstructure and properties of as-extruded and heat treated Mg-6Zn-1Mn-2Sn-0.5Ca alloy were investigated by optical microscopy (OM), X-ray diffractometer (XRD), scanning electron microscopy (SEM), transmission electron microscopy (TEM), hardness tests and uniaxial tensile tests.

## 1 Experiment

Billets were prepared with commercial purity Mg (>99.9 wt%), purity Zn (>99.95 wt%), purity Sn (>99.9 wt%), Mg-2.7Mn (2.7 wt%) and Mg-30Ca (30 wt%) master alloy. All the materials were melted at about 730 °C in a ZG-0.01 vacuum induction melting furnace in an Ar gas atmosphere. The actual chemical composition of Mg-5.62-0.91Mn-1.82Sn-0.48Ca (ZMT612-0.5Ca) was tested by XRF-800 CCDE X-ray fluorescence spectrometer. The ingots were then homogenized at 330 °C for 14 h and 420 °C for 2 h. Before extruding the ingots, both the ingots and extrusion die were heated to 350 °C for 60 min. The ingots were extruded at 350 °C with an extrusion ratio of 25:1 and a ram speed of 12 mm/s. Then the extruded bars were solution-treated at 420 °C for 2 h in air atmosphere followed by water quenching (T4). After solution treatment, the following artificial aging treatments (T6) were performed. The aging treatment was carried out at 180 °C from 0 h to 100 h. Hardness measurements were performed by a micro-Vickers apparatus under a load of 50 g.

Optical microscopy (OM, OLYMPUS LEXT OLS4000) and scanning electron microscopy (SEM, ESCAN VEGA II) equipped with energy dispersive X-ray spectrometer (EDS) observation was carried out. Phase analysis was determined by X-ray diffractometer (XRD, Rigaku D/max2500PC) using a Cu K $\alpha$  radiation with a scanning angle from 10° to 90° and a scanning rate of 4°/min. Tensile tests were carried out at room temperature using an

electronic universal testing machine (SANS CMT-5105) at a strain rate of  $\sim 1.43 \times 10^{-3} \text{ s}^{-1}$  with a gauge length of 35 mm and a cross-sectional diameter of 5 mm.

## 2 Results and Discussion

### 2.1 Microstructure of tested alloy

XRD patterns of the tested alloy in as-cast condition are shown in Fig.1. The phase for ZMT612-0.5Ca alloy includes  $\alpha$ -Mg, Mg<sub>7</sub>Zn<sub>3</sub>, Mn, Ca<sub>2</sub>Mg<sub>6</sub>Zn<sub>3</sub> and CaMgSn. The electronegative value of Mg, Zn, Sn, Ca are 1.31, 1.96, 1.65 and 1.00, respectively<sup>[15]</sup>. The electro-negativity difference between Ca and Sn is the highest among all the elements, implying that Ca and Sn are more likely to form CaMgSn ternary phase, so most Ca elements are consumed firstly by Sn. Then CaMgZn ternary phase is supposed to form. So intensity of peak of Ca<sub>2</sub>Mg<sub>6</sub>Zn<sub>3</sub> phase is low in XRD results. For the Mg-Zn-Ca alloy, Ca<sub>2</sub>Mg<sub>6</sub>Zn<sub>3</sub> phase instead of Mg<sub>2</sub>Ca is supposed to form when the Zn/Ca atomic ratio is higher than 1.23 according to the previous work<sup>[16]</sup>. In this study, Mn still remains as simple substance instead of compound. So the effect of Mn in this alloy is similar to that in Mg-6Zn-1Mn alloy<sup>[17]</sup>.

SEM images of the as-cast alloy are shown in Fig.2. White Mg<sub>7</sub>Zn<sub>3</sub> phases are parted by needle or feather-like phases which are distributed in grains or near grain boundaries. These needle or feather-like phases can be related to CaMgSn according to the EDS results in Table 1 and XRD results. According to the previous study<sup>[15]</sup>, CaMgSn phase co-exists with  $\alpha$ -Mg throughout all the solid phase regions at high temperature. As the temperature decreases, Ca<sub>2</sub>Mg<sub>6</sub>Zn<sub>3</sub> and MgZn phases appear.

Fig.3a shows the optical microstructures of tested alloy in the extruded condition (along extrusion direction (ED)). The as-extruded ZMT612-0.5Ca alloy presents a totally recrystallized microstructure, which indicates that complete dynamic recrystallization occurs during extrusion. The average grain size of extruded alloy is  $\sim 2.8 \mu\text{m}$ . Many second phases in micrometer are distributed along extrusion streamline. It is reported that the second phase particles with diameters over 1  $\mu\text{m}$  may act as nucleation sites<sup>[18]</sup>. In

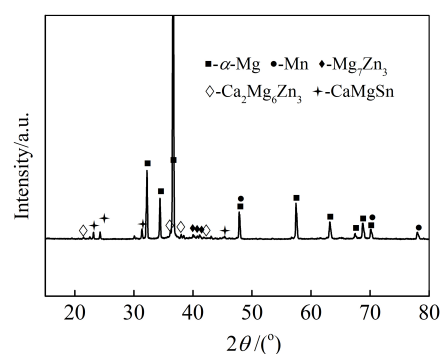


Fig.1 XRD pattern of as-cast alloy

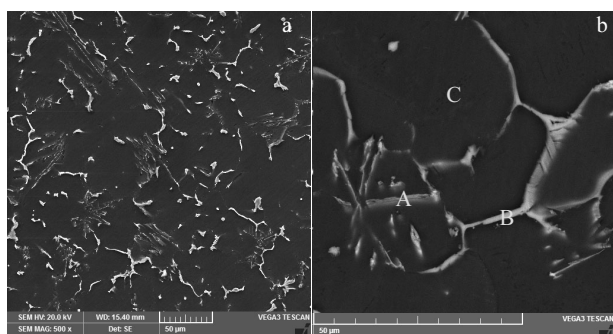


Fig.2 SEM images of microstructure of as-cast alloy

**Table 1 EDS results of the region of as-cast Mg-Zn-Mn-Sn-Ca alloy marked in Fig.2b (at%)**

Region	Mg	Zn	Ca	Sn	Mn
A	299	0.3	6.5	5.9	-
B	71.9	27.6	0.5	-	-
C	99.27	-	-	-	0.73

this study, the undissolved CaMgSn can act as nucleation sites during dynamic recrystallization, resulting in the heterogeneous deformation zone and promoting nucleation of recrystallization. This is known as particle stimulated nucleation (PSN)<sup>[19]</sup>. Therefore, there are many finer grains near second phases than other regions in Fig.3a. SEM image is shown in Fig.3b. Fine spherical and rod-shape second phases with an diameter much smaller than 1  $\mu\text{m}$  are densely distributed in grains and grain boundaries, which are identified as CaMgSn phase. Most CaMgSn phases cannot dissolve into  $\alpha$ -Mg and brake into particles along ED direction during extrusion. Particles with diameters less than 1  $\mu\text{m}$  distributed in grains and grain boundaries will act as barriers blocking dislocation and grain boundary movement. As a result, fined and homogenized structure is obtained after extrusion.

Fig.4 shows the microstructure of solution treated alloy at 420  $^{\circ}\text{C}$  for 2 h. XRD pattern of solution treated alloy is presented in Fig.5. Grain size increases obviously after solution, and most second phases are dissolved into Mg matrix. Only some dot-like phases still exist which can

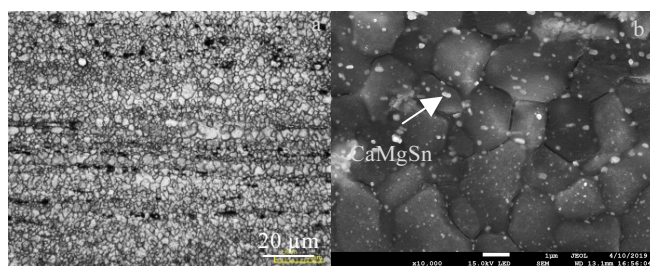


Fig.3 OM (a) and SEM (b) images of as-extruded alloy

prohibit grain growth during solution treatment. This result can also be obtained from XRD results that the peaks of Mg-Zn and  $\text{Ca}_2\text{Mg}_6\text{Zn}_3$  phase disappear totally. However, the diffraction peaks of CaMgSn phase are observed to be weakened but still exist, suggesting that a small number of CaMgSn cannot be dissolved into matrix at 420  $^{\circ}\text{C}$  because CaMgSn is a more thermally stable phase than Mg-Zn and  $\text{Ca}_2\text{Mg}_6\text{Zn}_3$ .

Fig.6 shows the TEM bright field (BF) images taken parallel to  $[11\bar{2}0]_{\text{Mg}}$  of ZMT612-0.5Ca alloy in peak aged condition at 180  $^{\circ}\text{C}$  for 10 h. The selected area electron diffraction (SAED) pattern of white circle region is also shown in this figure. Numbers of rod precipitates ( $\beta'$ ) parallel to  $[0001]_a$  direction and plate precipitates ( $\beta''$ ) perpendicular to  $[0001]_a$  are observed after aging treatment. These orientation relationships agree well with previous research<sup>[20,21]</sup>. CaMgSn particles are also found in Fig.6. Undissolved CaMgSn particles after solid solution can also provide the heterogeneities for nucleation of  $\beta'$  precipitation.

As we all know, basal slip is the major slippage mode for Mg alloys.  $\beta'$  is very helpful to block the dislocation movement on the base plane. So these phases are very important for aging hardening. While plate  $\beta''$  phase parallels to basal plane, so the ability of  $\beta''$  to block the dislocation movement is much weaker than that of  $\beta'$ . Besides, rod  $\beta'$  is finer than that in alloy ZMT614<sup>[10]</sup>, implying that  $\beta'$  is refined by the addition of Ca.

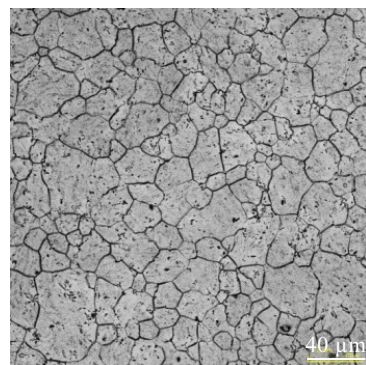
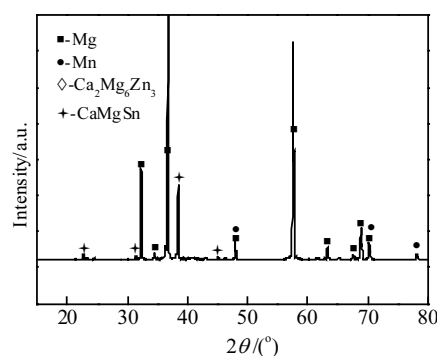
Fig.4 OM image of solution treated alloy at 420  $^{\circ}\text{C}$  for 2 h

Fig.5 XRD pattern of solution treated alloy

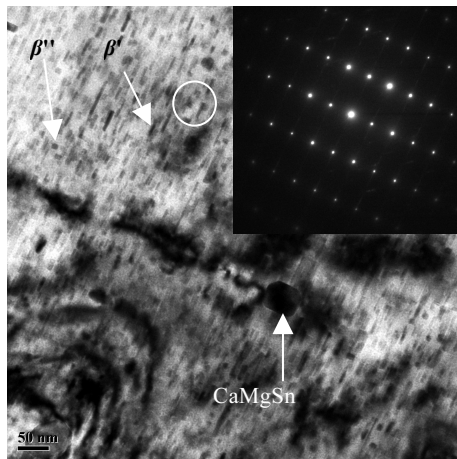


Fig.6 TEM-BF image taken parallel to  $[11\bar{2}0]_{Mg}$  of ZMT612-0.5Ca alloys peak aged at 180 °C for 10 h

## 2.2 Mechanical properties

Fig.7 shows the age-hardening curve of the solution-treated ZMT612-0.5Ca alloys during aging treatment at 180 °C. The hardness of this alloy after solution is ~730 MPa. The hardness reaches peak value (960 MPa) after ~10 h, and then declines gradually after 10 h. This means that the alloy undergoes over-aging stage.

Fig.8 and Table 2 show the mechanical properties of the test alloy in the as-extruded and peak aged conditions. For the as-extruded alloys, the YS (yield strength), UTS (ultimate tensile strength), and EL (elongation-to-failure) are 299 MPa, 366 MPa and 9.2%, respectively. Compared with ZMT614 and ZMT614-Y<sup>[22]</sup>, strength of tested alloy increases drastically, as shown in Table 2. For the peak aged alloys, the YS increases to 320 MPa and UTS increases to 390 MPa, while the EL decreases a little bit to 8.8%. It indicates that ZMT612-0.5Ca alloy responses well to aging treatment. Compared with ZMT614 and ZMT614-Y, the YS of tested alloy decreases while EL increases, implying that the strain hardening rate of the material in aging state is increased. This phenomenon may be related to the finer  $\beta'$ . The finer the phase, the easier the slip for Mg alloys.

The improvement of YS of ZMT612-0.5Ca after aging treatment is attributed to the grain boundary strengthening, solid solution strengthening and precipitation strengthening<sup>[23]</sup>. According to the Orowan equations, Zhu<sup>[24]</sup> and Starke<sup>[25]</sup> have established a widely used model to evaluate the precipitation strengthening of rod-shaped precipitates by computer aided simulation:

$$\Delta\sigma_p = 0.12 MG \frac{b}{2\sqrt{r}h} (f_v^{0.5} + 0.70(r/h)0.5f_v + 0.12(r/0.12(r/h)f_v^{1/2}) \cdot \ln(0.158r/r_0))$$

where  $\Delta\sigma_p$  is the increment of yield strength due to precipitation strengthening,  $M$  denotes the Taylor factor,  $G$  is

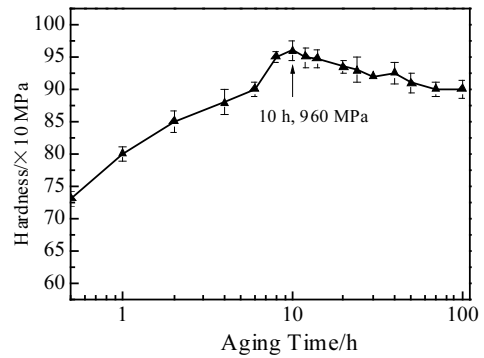


Fig.7 Aging-hardening curve of ZMT612-0.5Ca alloy at 180 °C

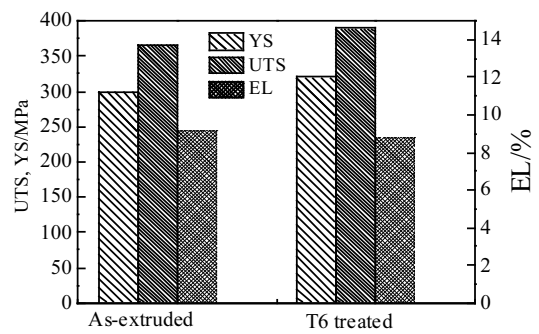


Fig.8 Mechanical properties of alloy in as-extruded and heat treated conditions

Table 2 Mechanical properties of tested alloy in as-extruded and heat treated conditions

	YS/MPa	UTS/MPa	EL/%
As-extruded	299	366	9.2 <sup>[this study]</sup>
	254	338	15.7 <sup>[22]</sup>
	259	350	18.3 <sup>[22]</sup>
Heat treated	320	390	8.8 <sup>[this study]</sup>
	353	367	5.27 <sup>[22]</sup>
	367	372	6.93 <sup>[22]</sup>

the shear modulus,  $t$  is thickness of particles,  $b$  is the magnitude of the Burgers vector;  $r$ ,  $h$  and  $f_v$  are the radius of habit plane, the half-thickness of peripheral plane and volume fraction of plate-shaped precipitates, respectively;  $r_0$  is the inner cut-off radius for the calculation of the dislocation line tension. If the shape of all the precipitates before and after aging is constant, the  $\Delta\sigma_p$  is dependent on  $f_v$ . The density of  $\beta'$  precipitates increases substantially in the peak aged condition, leading to the obvious increase of strength. However, the coarse CaMgSn

particles may act as crack initiation, so the EL of aged alloy decreases a little.

### 3 Conclusions

1) The as-cast ZMT612-0.5Ca alloy consists of  $\alpha$ -Mg,  $\text{Mg}_7\text{Zn}_3$ ,  $\text{Ca}_2\text{Mg}_6\text{Zn}_3$  and  $\text{CaMgSn}$  phases.

2) The as-extruded ZMT612-0.5Ca alloy presents a totally recrystallized microstructure. The average grain size of extruded alloy is  $\sim 2.8 \mu\text{m}$ .

3) A large number of  $\beta'$  rods may precipitate in the aging treatment process. The  $\beta'$  rods are parallel to the  $[0001]_a$ .

4) Compared with the as-extruded alloy, the ultimate tensile strength and yield strength of heat-treated alloy are increased to 390 and 320 MPa, respectively.

### References

- 1 You S H, Huang Y D, Kainer K U et al. *Journal of Magnesium and Alloys*[J], 2017(5): 239
- 2 Pan H C, Ren Y P, Fu H et al. *Journal of Alloys & Compounds*[J], 2016, 663: 321
- 3 Alaneme K K, Okotete E A. *Journal of Magnesium & Alloys*[J], 2017, 5(4): 460
- 4 Peng Q M, Dong H W, Wang L D et al. *Materials Science & Engineering A*[J], 2008, 477(1-2): 193
- 5 Sandlöbes S, Friák M, Zaefferer S et al. *Acta Materialia*[J], 2012, 60(6-7): 3011
- 6 Judit M, Pablo P, Gerardo G et al. *Materials Characterization*[J], 2017, 129: 195
- 7 Akihisa I, Yoshihito K, Mitsuhide M et al. *Journal of Materials Research*[J], 2001, 16(7): 1894
- 8 Chai Y F, Jiang B, Song J F et al. *Journal of Alloys and Compounds*[J], 2019, 482: 1076
- 9 Sasaki T T, Oh-Ishi K, Ohkubo T et al. *Materials Science & Engineering A*[J], 2011, 530: 1
- 10 Qi F G, Zhang D F, Zhang X H et al. *Journal of Alloys and Compounds*[J], 2014, 585: 656
- 11 Ali Y, Qiu D, Jiang B et al. *Journal of Alloys and Compounds*[J], 2015, 619: 639
- 12 Chang L L, Tang H, Guo J. *Journal of Alloys and Compounds*[J], 2017, 703: 552
- 13 Zhang Y, Song L P, Chen X Y et al. *Materials*[J], 2018, 11(9): 1490
- 14 Pan H C, Qin G W, Huang Y et al. *Acta Materialia*[J], 2018, 149: 350
- 15 Wahid S A, Lim H K, Jung Y G. *Journal of Korea Foundry Society*[J], 2018, 38(4): 75
- 16 Du Y Z, Qiao X G, Zheng M Y et al. *Materials & Design*[J], 2016, 98: 285
- 17 Zhang Dingfei, Qi Fugang, Shi Guoliang et al. *Rare Metal Materials and Engineering*[J], 2010, 39(12): 2205 (in Chinese)
- 18 Jiang L Y, Zhang D F, Fan X W et al. *Metal Science Journal*[J], 2015, 32(18): 1838
- 19 Humphreys F J. *Acta Metallurgica*[J], 1977, 25(11): 1323
- 20 Nie J F, Muddle B C. *Acta Materialia*[J], 2000, 48(8): 1691
- 21 Singh A, Tsai A. *Scripta Materialia*[J], 2007, 57(10): 941
- 22 Hu G S, Zhang D F, Zhao D Z et al. *Transactions of Nonferrous Metals Society of China*[J], 2014, 24(10): 3070
- 23 Zhang L, Gong M, Peng L M. *Materials Science and Engineering A*[J], 2013, 565: 262
- 24 Zhu A, Starke E A. *Acta Materialia*[J], 1999, 47(11): 3263
- 25 Nandy S, Kalyan K R. *Materials Science & Engineering A*[J], 2015, 644: 413

## Mg-6Zn-1Mn-2Sn-0.5Ca 合金挤压态和热处理态的组织与力学性能

陈霞<sup>1,2</sup>, 张丁非<sup>1,2</sup>, 冯靖凯<sup>1,2</sup>, 赵阳<sup>1,2</sup>, 蒋斌<sup>1,2</sup>, 潘复生<sup>2,3</sup>

(1. 重庆大学 材料科学与工程学院, 重庆 400044)

(2. 重庆大学 国家镁合金材料工程技术研究中心, 重庆 400044)

(3. 重庆市科学技术研究院, 重庆 401123)

**摘要:** 利用光学显微镜、X 射线衍射仪、扫描电镜、透射电镜、硬度以及力学性能测试仪等对挤压态和时效处理的 Mg-6Zn-1Mn-2Sn-0.5Ca 镁合金的显微组织和力学性能进行研究。结果表明: 合金铸态的相组成为  $\alpha$ -Mg, Mn,  $\text{Mg}_7\text{Zn}_3$ ,  $\text{Ca}_2\text{Mg}_6\text{Zn}_3$  和  $\text{CaMgSn}$  相。挤压态组织为完全动态再结晶组织, 晶粒尺寸约为  $2.8 \mu\text{m}$ 。固溶时效处理 (T6,  $180^\circ\text{C}+10\text{h}$ ) 后, 合金的强度明显增加, 屈服强度和抗拉强度分别为 320 和 390 MPa。合金强度的提高主要是由于晶界强化, 固溶强化和析出强化作用。

**关键词:** Mg-Zn-Mn-Sn-Ca; 挤压; 峰时效; 组织; 力学性能

作者简介: 陈霞, 女, 1990 年生, 博士, 重庆大学材料科学与工程学院, 重庆 400044, E-mail: chenxia13091025@163.com